

## Multi-analytical Techniques for the Study of Historical Pigments in the Painted Ceilings of Sadr Jahromi's House in Shiraz, Iran

D. Harandi<sup>\*1</sup>, M. Yari<sup>2</sup>

<sup>1</sup> Department of Conservation and Archaeometry, Faculty of Applied Arts, Tabriz Islamic Art University, P.O. Box: 15385-4567, Tabriz, Iran.

<sup>2</sup> Department of Archaeology, University of Tehran, P.O. Box: 141761-4411, Tehran, Iran.

### ARTICLE INFO

Article history:

Received: 09 July 2025

Final Revised: 03 Nov 2025

Accepted: 05 Nov 2025

Available online: 25 Apr 2026

Keywords:

Pigment identification

Historical pigments

Qajar period

Panel painting

Raman spectroscopy

### ABSTRACT

*This study investigates the pigments and materials employed in the wooden ceiling paintings discovered beneath the mirrorwork decorations of Sadr Jahromi's house in Shiraz. Multi-analytical techniques, including Raman spectroscopy, scanning electron microscopy coupled with energy-dispersive X-ray spectroscopy (SEM-EDX), optical microscopy, and Fourier-transform infrared spectroscopy (FTIR), were utilized to characterize the pigments and varnish. The analysis identified natural ultramarine blue, red lead, copper-based green (likely malachite), lead chromate, and white lead, either individually or in mixtures, within the painter's palette. Shellac was also used as a protective varnish for the painting. Moreover, SEM-EDX analysis revealed the presence of gold leaf applied beneath the paint layers. The findings suggest that the pigments used in these artworks date no earlier than the 19<sup>th</sup> century, reflecting the technical sophistication and artistic practices characteristic of the Qajar period. Prog Color Colorants Coat. 19 (2026), 375-387© Institute for Color Science and Technology.*

### 1. Introduction

Wood has been employed as an ideal substrate for the expression and creation of artistic works. Artists have used various pigments and techniques to increase their aesthetic appeal and creativity. The art of panel painting dates back thousands of years and reflects the cultural beliefs and aesthetic values of the past [1]. Such studies are essential for the conservation and restoration of these works. The characterization of pigments is crucial for documenting pigment preparation technology and identifying the materials used in the artist's palette [2].

Pigments and dyes have been extensively employed across various cultures, and the pigments used in these works have not only enhanced their beauty and visual appeal but also represent the technical and scientific advancements of the past [3]. Studies on historical pigments, such as Raman spectroscopy, a non-destructive

method, provide critical insights into the composition and origin of the materials used in these artworks [4]. The pigments and dyes used in painting on wood encompass a range of mineral pigments and organic dyes that contribute to the decoration of artistic works [5, 6].

Various studies have been conducted to identify the dyes and pigments used during the Qajar and Safavid periods. For instance, an investigation of two pen boxes (*Qalamdan*) from the Qajar era revealed the presence of ultramarine blue, chrome green, red lead, carbon black, and cochineal pigments used for decoration [7], furthermore, in a study aimed at identifying the pigments used in the painted wooden panels of the historical Shahsavaran House, dating back to the Qajar period, red lead, lead white, ultramarine, chrome yellow, and conicalcite were identified [8]. Addi-

\*Corresponding author: [\\*d.harandi@tabriziau.ac.ir](mailto:d.harandi@tabriziau.ac.ir),  
[daniel.harandi@gmail.com](mailto:daniel.harandi@gmail.com)

tionally, an analytical analysis of pigments of painting of wood from Qajar-era buildings identified pigments including blue lapis lazuli, red lead, huntite, and a mixture of carbon black and iron-based compounds as black pigments [9]. Additionally, in the identification of materials used in Qajar mural painting, the substrate layer was found to consist of a mixture of calcium sulfate and calcium carbonate. The red pigment was derived from red lead, while the green color was produced using a combination of malachite and Prussian blue. For the blue color, lapis lazuli was used accompanied by iron- and copper-based compounds [10].

The accurate identification of historical pigments in wood paintings presents a significant challenge. Many natural pigments employed in the past have undergone color changes or degradation over time, complicating their precise identification. These alterations are primarily driven by environmental factors such as humidity, light, and temperature, which have altered the chemical composition of the pigments over the centuries [1]. Furthermore, the lack of comprehensive documentation of artists' production processes and pigment compositions across different historical periods has hindered efforts to trace the exact origins of these materials and the methods of their application. Additionally, the use of locally sourced materials and varying access to natural resources have contributed to the considerable diversity of pigments across different geographical regions. Consequently, there is a pressing need for comprehensive, detailed research utilizing modern, non-destructive scientific techniques to identify and analyze these pigments. Such research not only enhances our understanding of art history and its techniques but also provides insights into the development of improved conservation strategies for this valuable cultural heritage [11].

Wood has been widely used in Iran to create various artworks and architectural structures. However, painting on wood became popular in Iran during the Safavid period. While studies have been conducted on the pigments used in Qajar artworks, such as wall paintings and manuscript decorations, research on wood painting has been relatively neglected. The historic Sadr Jahromi House is one of the most prominent architectural landmarks of the Qajar period in Shiraz. It belonged to

a notable and influential figure in the city. Its inscription as entry No. 2277 on Iran's National Heritage List reflects the building's architectural refinement and historical significance. This study, therefore, focuses on identifying the painting techniques employed in the late Qajar period, specifically in the ceiling of Sadr Jahromi's house in Shiraz. The research aims to identify the materials used in the wood decorations through analytical techniques.

## 2. Experimental

### 2.1. Materials and methods

Figure 1a shows the exterior view of the 19<sup>th</sup> century decorated house located in the southwestern city of Shiraz, Iran. The painted panels of this building were discovered during the restoration and preservation process (Figure 1c) beneath the mirrorwork decorations (Figure 1b) that had been applied in later periods over the original decorations.

Scanning Electron Microscopy (SEM) images and energy-dispersive X-ray spectra (EDX) were collected using a FE-SEM Tescan MIRA3 FEG-SEM (Czech) equipped with an EDAX spectrometer. Pigment samples were coated with gold, and SEM-EDX analyses were performed at an accelerating voltage of 15 kV without coating.

Raman spectra were acquired using a UNIDRON-A Raman microscope (Andor Technology) with a 532 nm diode laser, 50× objective, 20 mW power, 10 scans, 10 s acquisition time, and 2 cm<sup>-1</sup> spectral resolution. The Raman spectrum corresponding to each color was analyzed using the CHSOS (cultural heritage science open source) database as a reference for Raman spectra [12]. Optical light microscopy (OLYMPUS BX51, Japan) was used for preliminary identification of color structure and pigment combinations. Pigment powder was mounted on a glass slide with glycerin and observed at up to 200× magnification.

Fourier-transform infrared spectroscopy (FTIR, JASCO 680-plus, Japan) was conducted at room temperature (400-4000, 4 cm<sup>-1</sup> resolution, 32 scans). Samples from the coating layer were mixed with potassium bromide (KBr) and pressed at 6 bar to prepare pellets.



**Figure 1:** a) Sadr Jahromi's house in Shiraz, b and c) wooden panel painting discovered under mirrorwork during ceiling restoration, d and e) wooden panel painting of Sadr Jahromi's house and sampling locations, S1: Blue, S2: Red, S3: Green, S4: Yellow, S5: Metal leaf and substrate, S6: varnish.

### 3. Results and Discussion

#### 3.1. Red pigment

SEM-EDX microanalysis showed a Pb-rich element in the red color (Figure 3 a). Additionally, the presence of Al may be attributed to impurities. In general, the identification of artistic pigments is challenged by factors such as the presence of additional elements resulting from the artist's combination of different pigments, as well as coating resins and impurities that can occur over time or during sampling. These issues may complicate the accurate identification of the pigments. The red pigment shows significant similarities with the red lead reference spectrum obtained from the CHSOS Raman database [12]. Notably, distinctive bands at 138, 279, 345, and around the 540  $\text{cm}^{-1}$  [13]. demonstrate the use of red lead as a red pigment in painting (Figure 3b). In Figure 2, the red pigment is shown under PPL light. Lead (II, IV) oxide, under PPL, appears as pleochroic, translucent particles ranging from opaque orange to red, with high relief. In red lead, particle size ranges from very fine to medium-grained from sample to sample. As a result, particle shapes among samples appear rounded [1]. Red lead has been

used in paintings since ancient times and has been found in various types of artworks, including wall paintings, colorful sculptures, manuscript decorations, and canvas paintings. The term red lead is most commonly associated with the term "minium", which refers to the mineral  $\text{Pb}_3\text{O}_4$  [14].

#### 3.2. Blue pigment

Microscopic characteristics of the blue pigment were initially examined using optical microscopy. The Raman spectrum of the blue pigment closely matched that of ultramarine blue. A prominent peak at 543  $\text{cm}^{-1}$  corresponds to the symmetric stretching vibration of the  $S_3^-$  sulfur bond, while a weaker peak is associated with the  $S_2^-$  pigment in ultramarine Figure 5b [15]. The ultramarine blue pigment was identified by elemental analysis, which revealed the presence of sulfur and other elements, including aluminum and silicon. Additionally, the characteristic Raman bands at 1092 and 807  $\text{cm}^{-1}$  further confirmed the identity of the ultramarine blue pigment [16].

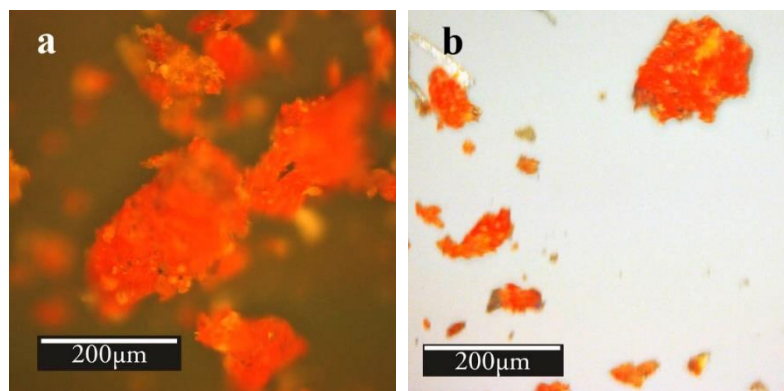


Figure 2: a) Reflective polarized light, b) Plane-polarized light microscopic images of red pigment.

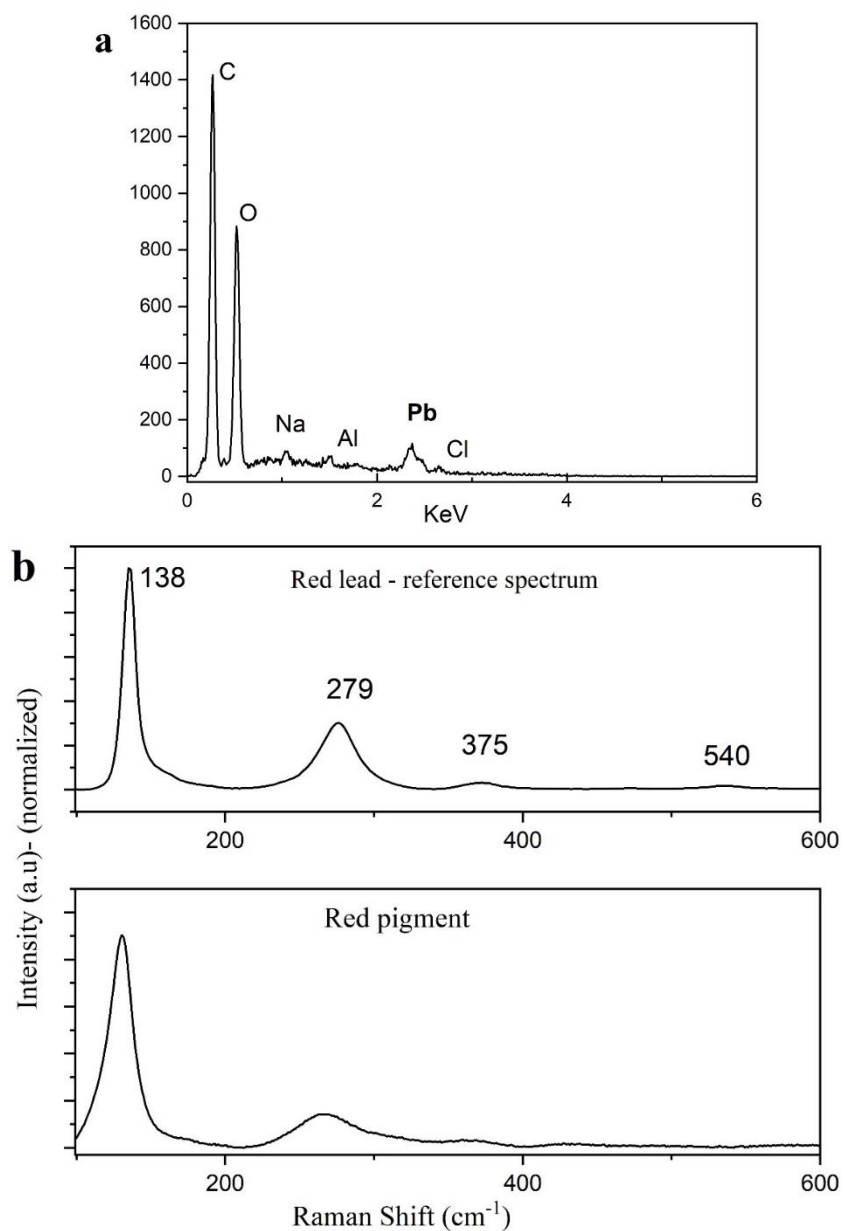


Figure 3: a) SEM-EDX analysis and b) Raman spectroscopy of red pigment.

As shown in the light microscope images, the blue pigment is accompanied by traces of red and white particles (Figure 4). The presence of impurities and variations in pigment composition poses a significant challenge to the identification of historical pigments. The presence of these red particles may be attributed to the artist's addition of red pigment to the color palette. However, the presence of red lead can be substantiated by the detection of Pb in SEM-EDS analysis and by characteristic Raman absorptions at 279 and 375  $\text{cm}^{-1}$ .

Natural ultramarine pigment is derived from lazurite, the blue mineral in lapis lazuli, and is crushed, ground, and purified as described by Cennini. Historically valued for its stability and vivid hue, it was extensively used in medieval European artworks. In general, ultramarine blue pigment is synthesized by burning sodium sulfate, quartz, and sulfur at approximately 800 °C, resulting in a sodium aluminum silicate sulfide ( $\text{Na}_8[\text{Al}_6\text{Si}_6\text{O}_{24}]\text{S}_n$ ). Synthetic ultramarine was first produced in 1828 by calcination and oxidation, replacing the natural form in the 19<sup>th</sup> century for its affordability while retaining its bright blue appearance [15, 16]. Natural ultramarine blue pigment, typically associated with impurities such as calcite ( $\text{CaCO}_3$ ), pyrite ( $\text{FeS}_2$ ), and possibly other minerals, constitutes a distinctive feature that differentiates natural ultramarine from synthetic. Based on SEM-EDS analysis, the pigment contained sulfur and calcite, indicating that the blue pigment is natural ultramarine [17]. Although its preparation and purification are described in Persian treatises, scientific analysis confirms the presence of natural lapis lazuli in

Iranian artwork from the medieval period (13<sup>th</sup>–14<sup>th</sup> centuries CE) to the Qajar era [18, 19].

### 3.3. Green pigment

The optical microscopy images are presented in Figure 6. As shown in the PPL image, the pigment is a mixture of green and yellow pigments, with trace amounts of white and blue particles. The combination of pigments is often a challenge in identifying historical pigments.

SEM-EDS analysis of the green pigment reveals a notable presence of Cu, indicating the use of a copper-based green pigment (Figure 7a). To achieve a more precise identification of the green pigments, Raman analysis was conducted (Figure 7b). The Raman spectrum of the green pigment shows similarity to the reference spectrum of malachite green pigment. The malachite pigment has characteristic peaks at 151, 178, 219, 270, 350, 430, 332, and 1095  $\text{cm}^{-1}$  [20, 21]. The bands at 536, 948, and 1420  $\text{cm}^{-1}$  are attributed to a (copper)acetate. Absorption due to  $\text{CO}_3^{2-}$  and  $\text{OH}^-$  ions of malachite appears at 720, 750, 1059  $\text{cm}^{-1}$  [22, 23]. As previously seen in the optical micrographs, the pigment consists of a mixture of several components and pigments, and the Raman spectrum exhibits additional peaks such as around 1000  $\text{cm}^{-1}$ , likely attributable to the presence of calcium-based fillers such as gypsum [24]. Additionally, the distinct peaks at 151, 975, 820, and 911  $\text{cm}^{-1}$  can be attributed to CuCl vibrations arising from malachite degradation products [25, 26].

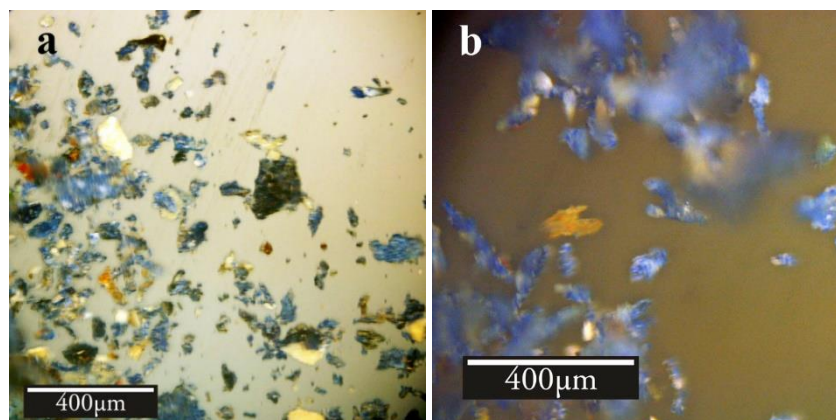
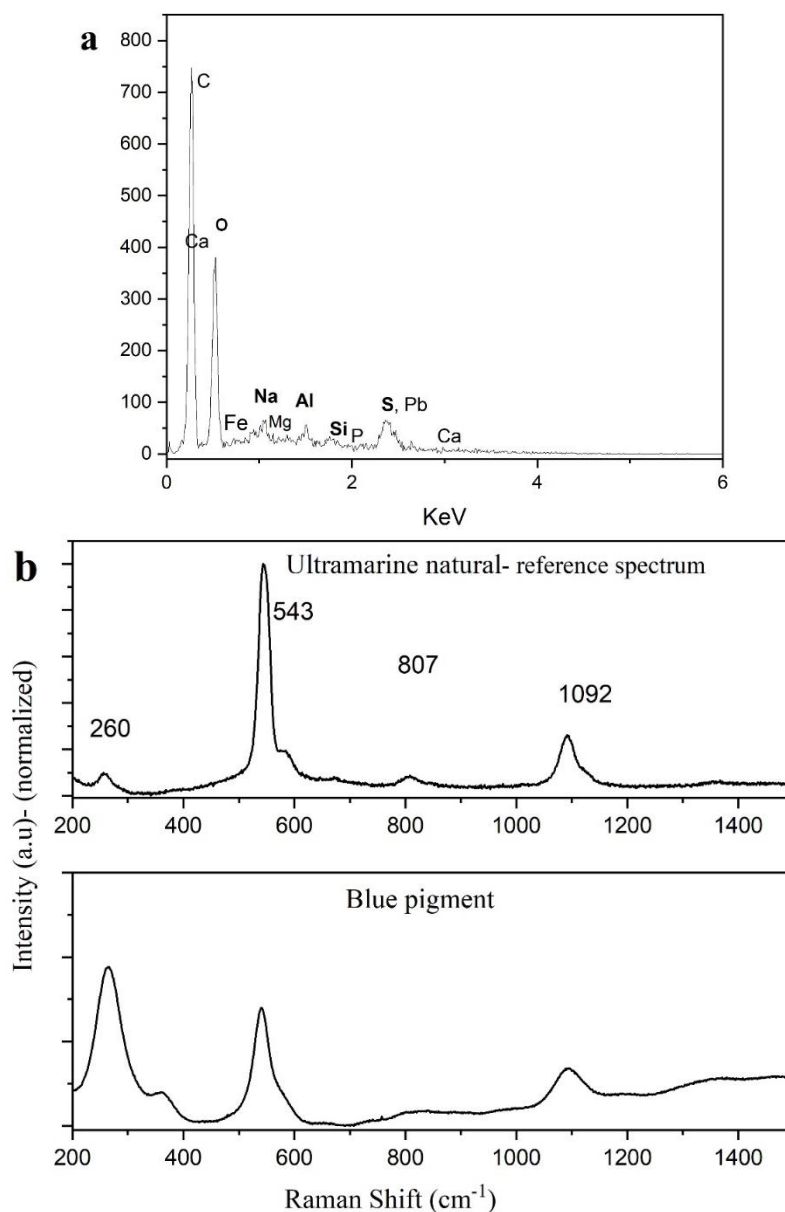


Figure 4: a) Plane-polarized light and b) Reflective polarized light microscopic image of blue pigment.



**Figure 5:** a) SEM-EDX analysis and, b) Raman spectroscopy of blue pigment and its correspondence with the reference spectrum of ultramarine blue pigment.

Malachite under optical microscopy exhibits a color range from light green to bright green, with its color intensity decreasing as particle size decreases. Malachite is a distinctive mineral when viewed under plane-polarised light, characterized by its green color, often with blue-green overtones, and pleochroic colours ranging from pale to mid-greens. The color intensity diminishes with smaller particle sizes, resulting in crushed malachite pigment that is typically coarse, though the particle size distribution may be uneven [1]. As a result, it can be said that malachite, a copper-based pigment, is used as a green pigment. Malachite has been used as a copper-based green pigment in historical

artwork, particularly in Iran. Malachite, known as copper carbonate ( $\text{Cu}_2\text{CO}_3(\text{OH})_2$ ), was one of several copper greens used alongside verdigris, atacamite, antlerite, and brochantite. The pigment was used primarily for floor tiles, architectural features, and clothing in Persian miniature paintings from the 16th and early 17th centuries [27]. A study of the green color used in Iranian architectural decorations from the 11th to the 15th centuries reported that, unlike malachite and verdigris, which were common in Persian manuscripts, atacamite was preferred for its durability against weathering [19].

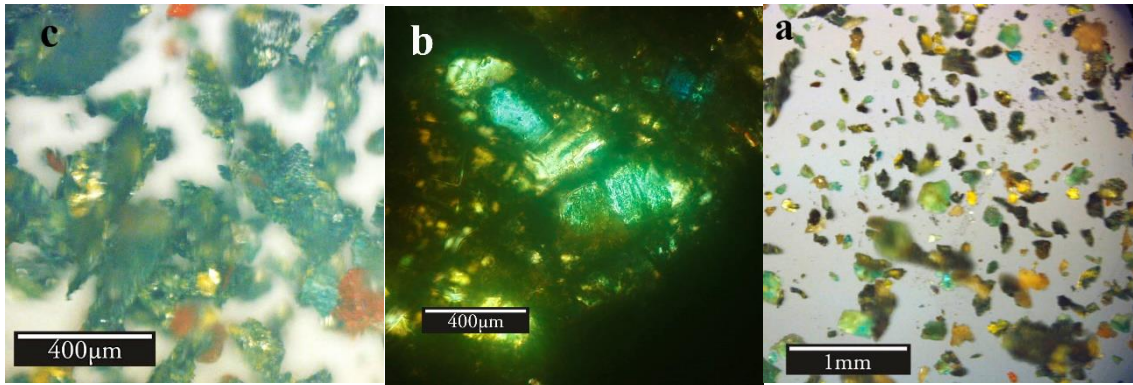


**Figure 6:** a) Plane-polarized light (PPL), b) cross-polarized light (XPL), and c) reflective polarized light microscopic images of green pigment.

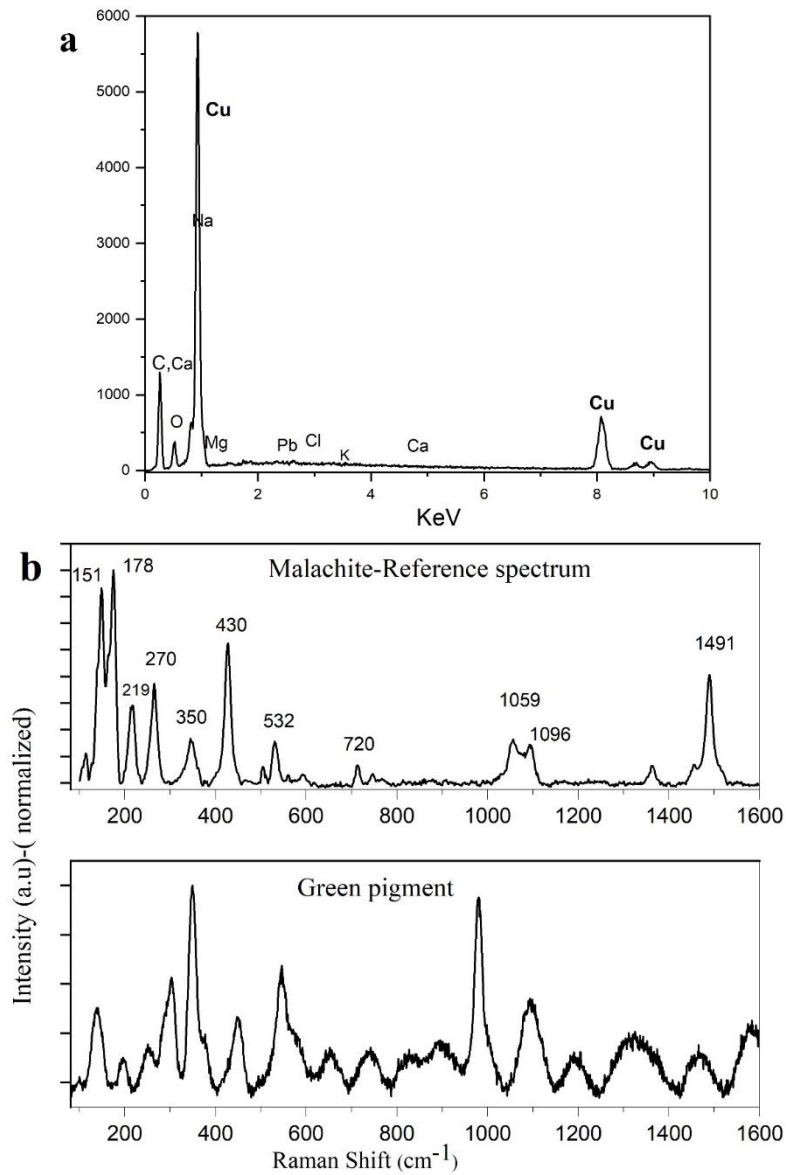


**Figure 7:** a) SEM-EDX analysis and b) Raman spectroscopy of green pigment and comparing with the reference Raman spectra of malachite pigment.

### 3.4. Yellow pigment

In Figure 8, microscopic images of yellow pigment under reflective polarized light and cross-polarized light are shown. Figure 9a presents the SEM-EDX spectrum of the yellow pigment, revealing the emission peaks of Cr and Pb. The identification of lead and chromium suggests the possible use of chrome yellow. In Figure 9b, the Raman spectrum of the pigment was compared with the reference spectrum of lead chromate. The bands at 351 and 838  $\text{cm}^{-1}$  (assigned to  $\nu_1$  symmetric stretching of the chromate ion) characteristic of lead chromate pigment are observed [28]. The bands at 351 and 838  $\text{cm}^{-1}$  have been shifted, which indicates photochemical degradation of chrome yellow. Previous studies have reported that structural changes and degradation products cause shifts towards lower wavenumbers and broadening of the Raman bands. These changes are caused by the photochemical conversion of Cr(VI) to Cr(III) [29]. Since the discovery of chromium in 1797 by Vauquelin and the synthesis of lead chromate in 1809, chrome yellow ( $\text{PbCrO}_4$ ) has been a notable addition to the 19th-century artist's palette [30, 31]. This color has been reported in a painting attributed to Kamal al-Molk, a 19<sup>th</sup>- and 20<sup>th</sup>-century Iranian painter [28].

### 3.5. Metal leaf, substrate and varnish on painting

Fourier-transform infrared spectroscopy (FTIR) was utilized to identify resin coating on the painting. The FTIR spectrum of the resin was compared with a shellac reference (Figure 10a). Shellac is a biodegradable resin composed of polyhydroxy acids, primarily aleuritic acid, shellolic acid, and jalaric acid, and other compounds [32]. The broad peak in the range of 3700-3200  $\text{cm}^{-1}$  corresponds to the O-H stretching of hydroxyl functional groups [33]. Absorption in the range of 2920-2980  $\text{cm}^{-1}$  results from C-H stretching. Additionally, carbonyl bands at 1710 and 1640  $\text{cm}^{-1}$  indicate the presence of C=O from shellac esters. In the fingerprint region (1500-500  $\text{cm}^{-1}$ ), key absorptions include 1462  $\text{cm}^{-1}$  ( $\text{CH}_2$  bending), 1374  $\text{cm}^{-1}$  ( $\text{CH}_3$  bending), 1250  $\text{cm}^{-1}$  (C-O stretching from ester), 1010 and 1000  $\text{cm}^{-1}$  (C-O stretching from alcohol), 943  $\text{cm}^{-1}$  (C-H stretching and  $\text{CH}_2$  wagging), and a weak peak at 720  $\text{cm}^{-1}$ , all of which are characteristic of shellac [34]. According to previous research by Poli et al. photo-oxidation products can be identified using FTIR spectroscopy. Comparison of the spectra of the reference shellac and the varnish from the artwork shows a decrease in the intensity of the 1520  $\text{cm}^{-1}$  band associated with ester groups, along with an increase in absorption intensity and a shift in the carbonyl group bands around 1650-1800  $\text{cm}^{-1}$ , indicating degradation and photo-oxidation processes in the historical varnish over time (Figure 10 b) [35].

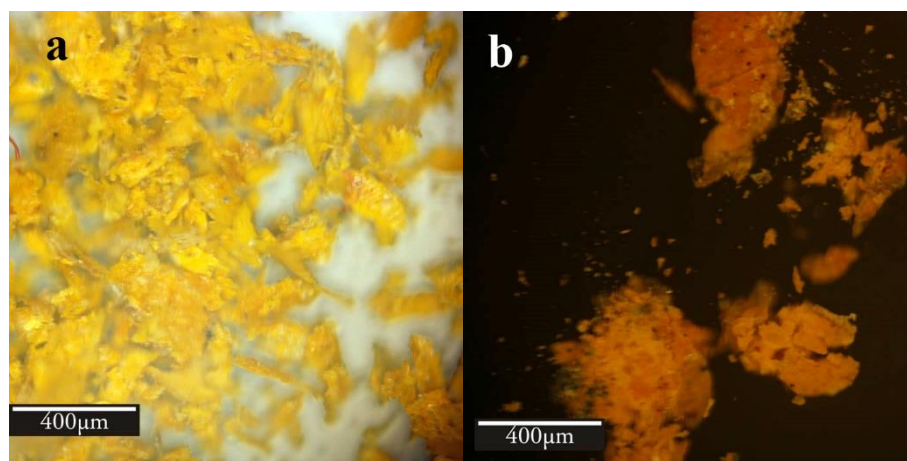


**Figure 8:** a) Reflective polarized light and b) Cross-polarized light microscopic images of yellow pigment.

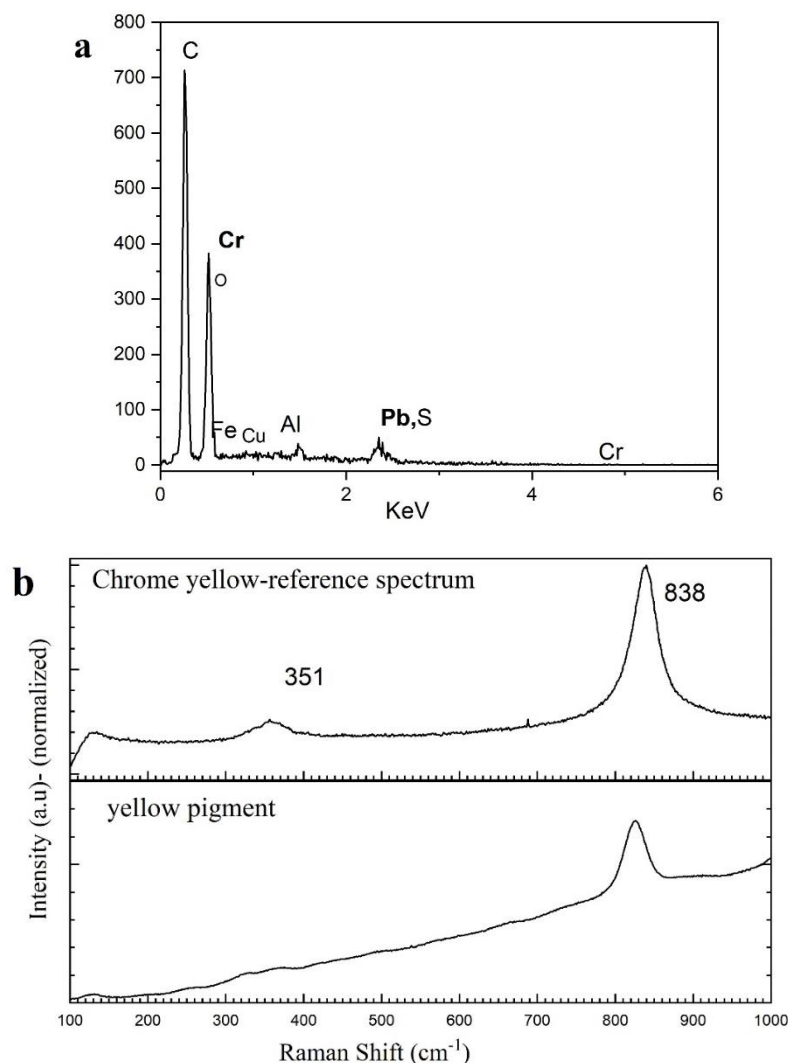


**Figure 9:** a) SEM-EDX analysis and b) Raman spectroscopy of yellow pigment and comparing it with the reference Raman spectrum of chrome yellow pigment.

Identification of alloys used in the thin metal leaf, such as gold leaf employed in different periods significantly improves our understanding of the materials and technology used in past. Figure 11a and b presents microscopic images of the placement of gold leaf beneath a paint layer. To determine the alloy composition of the gold leaf, SEM-EDX analysis revealed a high Au content in the gilding used on wooden paintings (Figure 11d). The application of gold leaf and the art of gilding have been widely used in Iranian decorative arts, employing various alloys for this purpose. For instance, during the Al-Muzaffar period, a distinct type of gold leaf containing with tin

and a transparent yellow coating was identified in the stucco decorations of the tomb of Sayyed Rukn ad-Din [36]. The SEM-EDX analysis of the sample substrate revealed elements such as C, O, Mg, Al, Si, Cl, Cu, and Pb (Figure 11c). Based on the elemental analysis (Table 1), the presence of lead (Pb) indicates the use of lead white, most likely basic lead carbonate ( $2\text{PbCO}_3 \cdot \text{Pb}(\text{OH})_2$ ). Furthermore, the detection of Ca, C, and O indicates the presence of calcium carbonate ( $\text{CaCO}_3$ ), which was likely used as a filler in the substrate. Minor amounts of Mg, Al, and Si are likely attributable to clay minerals and silicate impurities.

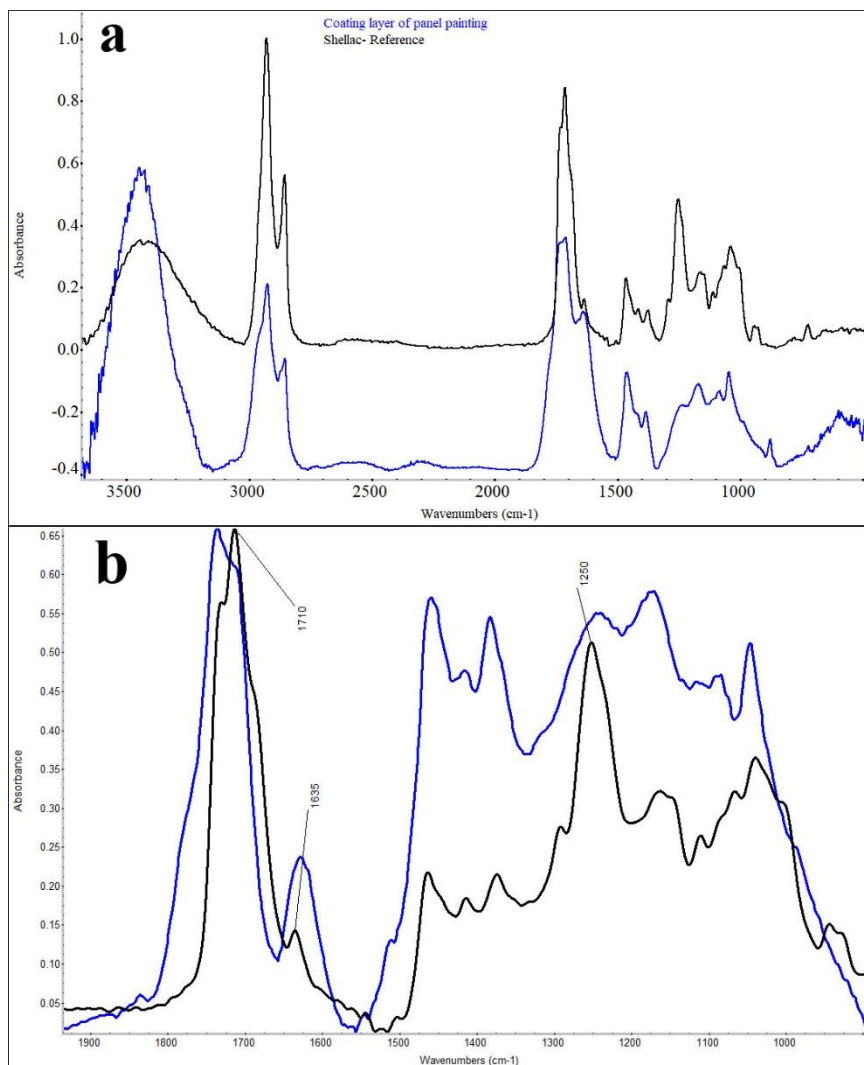


**Figure 10:** a) FTIR spectrum obtained of resin coated on the painting and comparing it with the Shellac reference FTIR spectrum and b) details of the range of 1900 and 900  $\text{cm}^{-1}$ .

**Table 1:** Elemental analysis results obtained from SEM-EDX.

Element %	C	O	Na	Mg	K	Al	Si	P	Pb	Ca	S	Cr	Fe	Cu	Au	Ag	Cl
Sample																	
Blue pigment	55.01	34.30	0.66	1.16	--	1.37	0.93	0.41	2.66	0.12	3.10	---	0.28	--	---	--	0.32
Red pigment	50.58	41.22	1.75	--	--	1.16	--	--	4.80	--	--	0.24	---	0.48	---	--	0.49
Green pigment	40.28	6.26	2.20	--	0.15	--	--	--	0.50	0.17	---	---	50.00	---	---		0.19
Yellow pigment	54.31	40.73		--	--	0.82	--	--	2.60	--	0.17	0.22	0.34	0.81	--		
substrate	69.01	10.88		1.93	--	1.58	2.64	--	4.96	2.50	--	--	--	3.68		4.96	--
Metal leaf	57.69	30.25	0.52	0.45	0.08	0.68	--	--	--	0.07	0.56	--	--	0.51	9.06	--	0.12

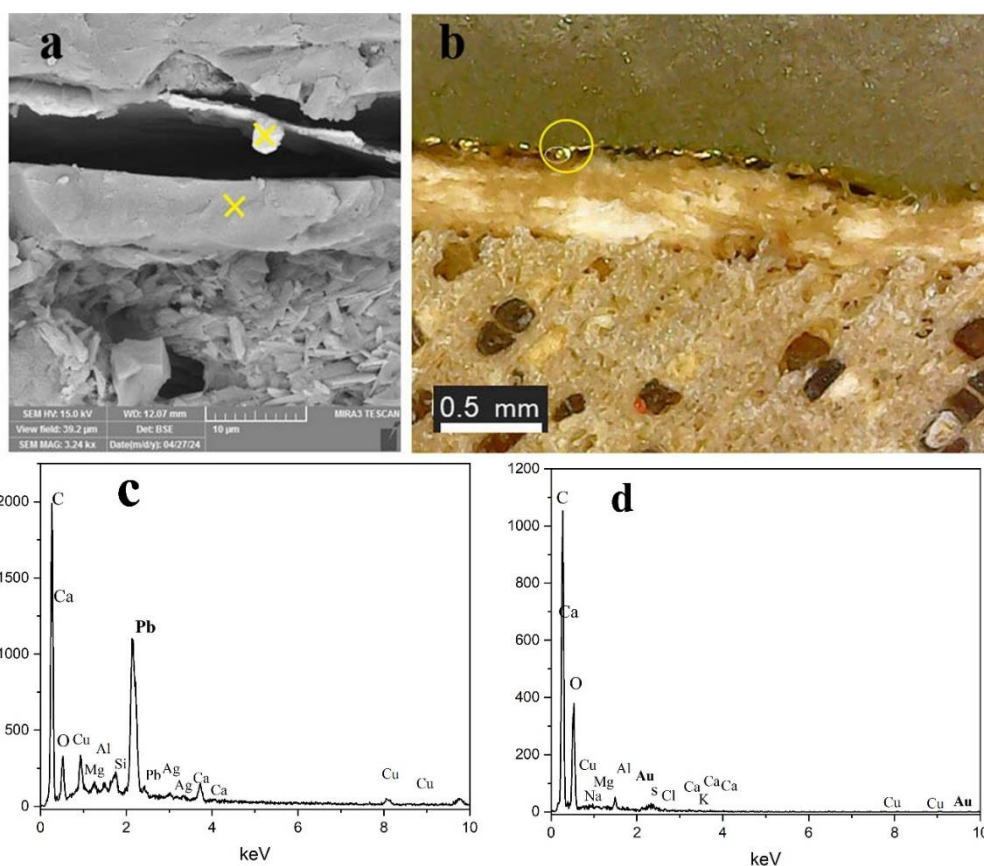


**Figure 11:** a) and b) SEM and digital microscopic images from cross-section of the painting layer, respectively, c) and d) SEM-EDX analysis of substrate and gold leaf, respectively.

#### 4. Conclusion

A multi-technique approach, including optical microscopy, Raman spectroscopy, X-ray spectroscopy, and infrared spectroscopy, was employed to analyze the materials used in the panel painting. The analysis revealed the presence of natural ultramarine blue, red lead, and chrome yellow as principal colorants in the artist's palette. A copper-based compound, possibly malachite, was applied to achieve a green color. According to the study, the artist predominantly used lead white to alter the painting's tonal variations. The gold leaf was identified on a white lead substrate, a common material for the decoration of wealthy people. Shellac resin was also applied as a protective coating over the paintings. The findings suggest that the painted

panels date to the building's 19<sup>th</sup> century construction period. In subsequent periods, these panels were dismantled and repurposed as an underlayer beneath the mirrorwork, with the paintings arranged without regard to their original design and pattern.

#### Acknowledgments

The authors extend our heartfelt gratitude to Mr. Esmail Hessampour, the esteemed cultural heritage official of Shiraz, for his invaluable support in providing the wooden panels that were integral to this study. His assistance greatly contributed to the successful completion of our research, and we deeply appreciate his dedication to the advancement of cultural heritage studies of Shiraz.

#### 5. References

1. Eastaugh N, Walsh V, Chaplin T, Siddall R. Pigment compendium: a dictionary of historical pigments: Routledge; 2007.
2. Stanzani E, Bersani D, Lottici PP, Colomban P.

Analysis of artist's palette on a 16th century wood panel painting by portable and laboratory Raman instruments. *Vibrational Spect.* 2016; 85:62-70. <https://doi.org/10.1016/j.vibspec.2016.03.027>.

3. Ball P. *Bright earth: art and the invention of color*. University of Chicago Press; 2003.
4. Cucci C, Delaney JK, Picollo M. Reflectance hyperspectral imaging for investigation of works of art: old master paintings and illuminated manuscripts. *Accounts Chem Res.* 2016; 49(10):2070-9. <https://doi.org/10.1021/acs.accounts.6b00048>.
5. Rostami-Charati F, Rahmani G, Bahadori R, Madani FS. A spectroscopic and nondestructive analysis methods for investigation of inorganic pigments in a cultural heritage in north of Iran. *Wood Res J.* 2021; 12(1):1-9.
6. Cartechini L, Miliani C, Nodari L, Rosi F, Tomasin P. The chemistry of making color in art. *J Cultural Herit.* 2021;50:188-210. <https://doi.org/10.1016/j.culher.2021.05.002>.
7. Koochakzai A, Marefat-Izady P. Application of micro-Raman spectroscopy for identifying pigments in qajar papier-mache penboxes (qalamdan). *J Color Sci Technol.* 2024;18(1):57-66. <https://dor.isc.ac/dor/20.1001.1.17358779.1402.18.1.5.7>
8. Koochakzai A, Mohammadi Achachluei M, Borzouyan M. A micro-analytical approach for pigments identification on qajarid wooden panels in Isfahan: identification of conicalcrite as a degradation product of emerald green. *Prog Color Colorant Coat.* 2024; 18(1):73-85. <https://doi.org/10.30509/pccc.2024.167302.1294>.
9. Hamzavi Y, Harandi D, Niazi F, Haji Seyyed Javadi SM. An investigation into the characterization of the painted wooden shir-sar of taqavi house in Gorgan. *Iranian J Wood Paper Sci Res.* 2024; 39(3):210-30.
10. Abbasi J, Bahadori R, Bozorgmehr MA, Beheshti SI, Bahrololoumi F. Identification of materials and pigments used in mural painting of Rahim Abad historic garden & mansion in Birjand. *J Res Archaeol.* 2017; 2(2):63-76. <https://doi.org/10.22092/ijwpr.2024.365427.1772>.
11. Gettens RJ, Stout GL. *Painting materials: a short encyclopedia*. Courier Corporation; 2012.
12. Cultural Heritage Science Open Source (CHSOS). *FREE Spectra Databases. Pigments Checker v.5.* 2019. Available from: <https://chsopensource.org/>.
13. Li Y, Ma J, He K, Wang F. Raman study of 532-nanometer laser-induced degradation of red lead. *Materials.* 2024;17(4):770. <https://doi.org/10.3390/ma17040770>.
14. Aze S, Vallet J-M, Detalle V, Grauby O, Baronnet A. Chromatic alterations of red lead pigments in artworks: a review. *Phase Transitions.* 2008;81(2-3):145-54. <https://doi.org/10.1080/01411590701514326>.
15. Osticioli I, Mendes N, Nevin A, Gil FP, Becucci M, Castellucci E. Analysis of natural and artificial ultramarine blue pigments using laser induced breakdown and pulsed Raman spectroscopy, statistical analysis and light microscopy. *Spectrochim Acta Part A: Mol Biomol Spect.* 2009;73(3):525-31. <https://doi.org/10.1016/j.saa.2008.11.028>.
16. Holakoei P, Karimy A-H, Vaccaro C. A multi-analytical approach to the examination of nineteenth-century European wallpapers in Vasiq-Ansari House in Isfahan, Iran. *Stud Conservat.* 2014; 59(3):150-60. <https://doi.org/10.1179/2047058413Y.0000000091>.
17. Darzi M, Stern B, Edwards HG, Surtees A, Rachti ML. A study of colourant uses in illuminated Islamic manuscripts from the Qajar period (1789–1925 CE), early modern Iran. *J Archaeol Sci: Report.* 2021; 39:103119. <https://doi.org/10.1016/j.jasrep.2021.103119>.
18. Purinton N, Waiters M. A study of the materials used by medieval Persian painters. *J Am Instit Conserv.* 1991;30(2):125-44. <https://doi.org/10.1179/019713691806066728>.
19. Holakoei P, Karimy AH. Colourants on the Persian architectural decorations from the 11th to the 15th century. *Archaeometry.* 2024;66(3):600-17. <https://doi.org/10.1111/arcm.12951>.
20. Marucci G, Beeby A, Parker AW, Nicholson C. Raman spectroscopic library of medieval pigments collected with five different wavelengths for investigation of illuminated manuscripts. *Anal Method.* 2018;10(10):1219-36. <https://doi.org/10.1039/C8AY00016F>.
21. Coccato A, Bersani D, Coudray A, Sanyova J, Moens L, Vandenberghe P. Raman spectroscopy of green minerals and reaction products with an application in Cultural Heritage research. *J Raman Spect.* 2016; 47(12):1429-43. <https://doi.org/10.1002/jrs.4956>.
22. De Laet N, Lycke S, Van Pevenage J, Moens L, Vandenberghe P. Investigation of pigment degradation due to acetic acid vapours: Raman spectroscopic analysis. *European J Mineral.* 2013;25(5):855-62. <https://doi.org/10.1127/0935-1221/2013/0025-2298>.
23. Bouchard M, Smith DC. Catalogue of 45 reference Raman spectra of minerals concerning research in art history or archaeology, especially on corroded metals and coloured glass. *Spectrochim Acta Part A: Mol Biomol Spect.* 2003;59(10):2247-66. [https://doi.org/10.1016/S1386-1425\(03\)00069-6](https://doi.org/10.1016/S1386-1425(03)00069-6).
24. Bersani D, Lottici PP. Raman spectroscopy of minerals and mineral pigments in archaeometry. *J Raman Spect.* 2016;47(5):499-530. <https://doi.org/10.1002/jrs.4914>.
25. Kwon H, Kim L. On-site identification of corrosion products and evaluation of the conservation status of copper alloy artworks using a portable Raman spectrometer. *Materials.* 2025;18(5):924. <https://doi.org/10.3390/ma18050924>.
26. Frost RL. Raman spectroscopy of selected copper minerals of significance in corrosion. *Spectrochim Acta Part A: Mol Biomol Spect.* 2003;59(6):1195-204. [https://doi.org/10.1016/S1386-1425\(02\)00315-3](https://doi.org/10.1016/S1386-1425(02)00315-3).
27. Knipe P, Eremin K, Walton M, Babini A, Rayner G. Materials and techniques of Islamic manuscripts. *Heritage Sci.* 2018;6:1-40. <https://doi.org/10.1186/s40494-018-0217-y>.
28. Roohi S, Holakoei P. Art historical and scientific controversies about four easel paintings attributed to Kamal al-Molk, the renowned nineteenth-twentieth

- century Persian painter. *Heritage Sci.* 2023;11(1):197. <https://doi.org/10.1186/s40494-023-01033-z>.
29. Monico L, Janssens K, Miliani C, Brunetti BG, Vagnini M, Vanmeert F, et al. Degradation process of lead chromate in paintings by Vincent van Gogh studied by means of spectromicroscopic methods. 3. Synthesis, characterization, and detection of different crystal forms of the chrome yellow pigment. *Analyt Chem.* 2013;85(2):851-9. <https://doi.org/10.1021/ac102424h>.
30. Otero V, Carlyle L, Vilarigues M, Melo MJ. Chrome yellow in nineteenth century art: historic reconstructions of an artists' pigment. *RSC advances.* 2012;2(5):1798-805.
31. Edwards HG. Analytical Raman spectroscopic discrimination between yellow pigments of the Renaissance. *Spectrochim Acta Part A: Mol Biomol Spect.* 2011;80(1):14-20. <https://doi.org/10.1039/C1R A00614B>.
32. Irimia-Vladu M, Głowacki ED, Schwabegger G, Leonat L, Akpınar HZ, Sitter H, et al. Natural resin shellac as a substrate and a dielectric layer for organic field-effect transistors. *Green Chem.* 2013; 15(6): 1473-6. <https://doi.org/10.1039/C3GC40388B>.
33. Barik A, Patnaik T, Parhi P, Swain S, Dey R. Synthesis and characterization of new shellac-hydroxypropyl-methylcellulose composite for pharmaceutical applications. *Poly Bullet.* 2017; 74:3467-85. <https://doi.org/10.1007/s00289-017-1903-8>.
34. Yan G, Cao Z, Devine D, Penning M, Gately NM. Physical properties of shellac material used for hot melt extrusion with potential application in the pharmaceutical industry. *Polymers.* 2021;13(21):3723. <https://doi.org/10.3390/polym13213723>.
35. Poli T, Piccirillo A, Zoccali A, Conti C, Nervo M, Chiantore O. The role of zinc white pigment on the degradation of shellac resin in artworks. *Poly Degrad Stability.* 2014; 102:138-44.
36. Hamzavi Y, Salahshor F, Mozafar F. Gilding of plaster decorations in the tomb of sayyid rokn al-din in Yazd. *Islamic Art Studies.* 2013;19(10):39-46. <https://doi.org/10.1016/j.polymdegradstab.2014.01.026>.

How to cite this article:

Harandi D, Yari M. Multi-analytical Techniques for the Study of Historical Pigments in the Painted Ceilings of Sadr Jahromi's House in Shiraz, Iran. *Prog Color Colorants Coat.* 2026;19(4):375-387. <https://doi.org/10.30509/pccc.2025.167593.1418>.

